

## Theoretical study on the electronic states of NaLi

Ioannis D. Petsalakis, Demeter Tzeli, and Giannoula Theodorakopoulos<sup>a)</sup>

Theoretical and Physical Chemistry Institute, The National Hellenic Research Foundation, 48 Vassileos Constantinou Ave., Athens 116 35, Greece

(Received 21 May 2008; accepted 18 June 2008; published online 4 August 2008)

Configuration interaction calculations have been carried out on electronic states of the NaLi molecule and the cation NaLi<sup>+</sup>. Potential energy curves are presented for the lowest nine <sup>1</sup>Σ<sup>+</sup>, seven <sup>1</sup>Π, four <sup>1</sup>Δ, eight <sup>3</sup>Σ<sup>+</sup>, seven <sup>3</sup>Π, and four <sup>3</sup>Δ states of NaLi as well as for the lowest ten <sup>2</sup>Σ<sup>+</sup>, six <sup>2</sup>Π, and two <sup>2</sup>Δ states of NaLi<sup>+</sup>. The results of the present many-electron configuration interaction calculations on the cation are in support of previous core-polarization effective potential calculations. The present calculations on the NaLi molecule are complementary to previous theoretical work on this system, including recently observed electronic states that had not been calculated previously as well as an investigation of nonadiabatic effects leading to spectral perturbations. Furthermore, *ab initio* potential energy curves of the neutral and the ground state of the cation are employed to determine quantum defect that may be employed to generate potential energy curves for *nd* and *(n+1)p* (for *n* > 3) Rydberg states of NaLi. The present results on the 3 <sup>1</sup>Π and 4 <sup>1</sup>Π states are in good agreement with recent experimental work, whereas on the basis of theoretical data, the recently observed state 5 <sup>1</sup>Π is better described as 6 <sup>1</sup>Π. © 2008 American Institute of Physics. [DOI: 10.1063/1.2956510]

### I. INTRODUCTION

The electronic structure of the heteronuclear diatomic alkali molecule NaLi, with only two valence electrons, has been the object of theoretical studies by different methods including *ab initio*<sup>1-4</sup> and combination of *ab initio* with effective-core-polarization potentials.<sup>5-7</sup> In particular, in one of the previous studies on a large number of electronic states of NaLi, core-polarization potentials have been used to account for core-valence as well as intracore correlations, in all-electron self-consistent field plus valence (i.e., two-electron) configuration interaction (CI) calculations, with excellent results on the spectroscopic constants and vibrational levels of NaLi.<sup>6</sup> Corresponding experimental data have been relatively scarce because of difficulties caused by the overlap of the spectra of NaLi with those of Na<sub>2</sub>, with the first observation of NaLi, involving fluorescence spectra *B* <sup>1</sup>Π → *X* <sup>1</sup>Σ<sup>+</sup>, reported only in 1971.<sup>8</sup> Subsequently and until 1991 a number of experimental studies have appeared, including a mass spectrometric study yielding information on the dissociation energy and ionization potential (IP) of the ground state,<sup>9</sup> a laser induced fluorescence investigation of the *B* <sup>1</sup>Π → *X* <sup>1</sup>Σ<sup>+</sup> system,<sup>10</sup> as well as detection of the excited *A*(2)<sup>1</sup>Σ<sup>+</sup>, *C*(3)<sup>1</sup>Σ<sup>+</sup>, *D*(2)<sup>1</sup>Π, *E*(4)<sup>1</sup>Σ<sup>+</sup>, and *F*(5)<sup>1</sup>Σ<sup>+</sup> states.<sup>11</sup> A high-resolution spectroscopic study devoted to the *A* <sup>1</sup>Σ<sup>+</sup> → *X* <sup>1</sup>Σ<sup>+</sup> system,<sup>12</sup> observation of the electronic transitions *B* <sup>1</sup>Π → *A* <sup>1</sup>Σ<sup>+</sup> and *C* <sup>1</sup>Σ<sup>+</sup> → *A* <sup>1</sup>Σ<sup>+</sup>,<sup>13</sup> and high-accuracy determination of rotational-vibrational levels of the ground state<sup>14</sup> have been also reported. The vibrational-rotational levels of *B* <sup>1</sup>Π and *C* <sup>1</sup>Σ<sup>+</sup> are found to be perturbed, and this has been attributed to interactions between *B* <sup>1</sup>Π and *C* <sup>1</sup>Σ<sup>+</sup>.<sup>13</sup> Excellent agreement was found between experi-

mental spectroscopic constants, and in some cases, the vibrational levels of the states treated in the above experimental studies and the theoretical values of Schmidt-Mink *et al.*<sup>6</sup> Recently, new spectroscopic works on the *E*(4)<sup>1</sup>Σ<sup>+</sup> state<sup>15,16</sup> and spectra assigned to transitions from the ground state to 3 <sup>1</sup>Π and 4 <sup>1</sup>Π have been reported,<sup>17</sup> as well as spectra assigned to the 5 <sup>1</sup>Π state of NaLi.<sup>18</sup> This new experimental work on the higher-lying <sup>1</sup>Π states has shown the need for further theoretical work on the electronic states of NaLi, since the previous work<sup>6</sup> involved potential energy curves and vibrational levels of the <sup>1</sup>Σ<sup>+</sup> states of NaLi up to 6 <sup>1</sup>Σ<sup>+</sup>, as well as for a number of triplet states, but only for the lowest two <sup>1</sup>Π states. It is thus of interest to calculate in the present work the potential energy curves of the electronic states of the NaLi molecule and, in particular, of the higher-lying <sup>1</sup>Π states, which have not been calculated previously. In the present work a many-electron CI calculation method will be employed; as such calculations are feasible with present day computers. Second, nonadiabatic interactions between the different singlet states and the possible spectral perturbations are investigated. Third, the *ab initio* potential energy curves of the Na 3*d* and Na 4*p* <sup>1</sup>Π Rydberg states are employed along that of the ground state of the cation NaLi<sup>+</sup> in order to determine quantum-defect functions, useful for the generation of potential energy curves of higher-lying Rydberg states, up to the ionization limit, through quantum-defect calculations. Finally, along with the ground state of NaLi<sup>+</sup>, required for the quantum-defect calculations, potential energy curves of the excited states of the cation have been also calculated, in view of the fact that there have been no previous many-electron calculations on this system. There have been model potential calculations on the electronic states of NaLi<sup>+</sup>, which are in good agreement (but the agreement is in part artificial as stated by the authors<sup>19</sup>) with avail-

<sup>a)</sup>Electronic mail: ithe@eie.gr.

TABLE I. Excitation energies ( $\text{cm}^{-1}$ ) of  $\text{NaLi}^+$  and  $\text{NaLi}$  at the dissociation limits [at  $R=50.0$  bohr for  $\text{NaLi}$  and  $100.0$  bohr for  $\text{NaLi}^+$ ].

State	$\Delta E_{\text{th}}$ (present work)	$\Delta E_{\text{exp}}^{\text{a}}, \Delta E_{\text{th}}^{\text{b}}$
<b>(a) <math>\text{NaLi}^+</math></b>		
[Na $4p+\text{Li}^+$ ] $10^2\Sigma^+, 6^2\Pi$	321 80, 321 97	323 05, 323 09
[ $\text{Na}^++\text{Li } 3d$ ] $9^2\Sigma^+, 5^2\Pi, 2^2\Delta$	317 31, 317 61, 317 57	312 83, 312 86
[Na $3d+\text{Li}^+$ ] $8^2\Sigma^+, 4^2\Pi, 1^2\Delta$	315 56, 315 56, 315 50	312 11, 312 11
[ $\text{Na}^++\text{Li } 3p$ ] $7^2\Sigma^+, 3^2\Pi$	309 81, 310 14	309 25, 309 26
[Na $4s+\text{Li}^+$ ] $6^2\Sigma^+$	276 89	277 78, 277 76
[ $\text{Na}^++\text{Li } 3s$ ] $5^2\Sigma^+$	271 80	272 06, 272 12
[Na $3p+\text{Li}^+$ ] $4^2\Sigma^+, 2^2\Pi$	189 28, 189 35	189 94, 190 04
[ $\text{Na}^++\text{Li } 2p$ ] $3^2\Sigma^+, 1^2\Pi$	149 96, 150 16	149 03, 149 05
[Na $3s+\text{Li}^+$ ] $2^2\Sigma^+$	2244	2038 (434 87), 2037
[ $\text{Na}^++\text{Li } 2s$ ] $X^2\Sigma^+$	0 (411 35)	0 (414 49)
<b>(b) <math>\text{NaLi}</math></b>		
[Na $3p+\text{Li } 2p$ ]		
$10^1\Sigma^+, 7^1\Pi, 3^1\Delta, 1^1\Sigma$	319 54, 319 22, 319 35, 319 37	
$10^3\Sigma^+, 7^3\Pi, 3^3\Delta, 1^3\Sigma^-$	319 64, 320 13, 318 12, 319 74	318 60
[Na $3s+\text{Li } 3d$ ] $9^1\Sigma^+, 6^1\Pi, 2^1\Delta, 9^3\Sigma^+, 6^3\Pi, 2^3\Delta$	318 55, 318 65, 315 83, 319 44, 319 38, 315 86	312 83
[Na $3s+\text{Li } 3p$ ] $8^1\Sigma^+, 5^1\Pi, 8^3\Sigma^+, 5^3\Pi$	311 30, 310 78, 311 32, 311 40	309 25
[Na $4p+\text{Li } 2s$ ] $7^1\Sigma^+, 4^1\Pi, 7^3\Sigma^+, 4^3\Pi$	300 24, 299 38, 300 28, 299 54	302 67
[Na $3d+\text{Li } 2s$ ] $6^1\Sigma^+, 3^1\Pi, 1^1\Delta, 6^3\Sigma^+, 3^3\Pi, 1^3\Delta$	294 38, 294 23, 294 55, 294 64, 294 39, 294 68	291 73
[Na $3s+\text{Li } 3s$ ] $5^1\Sigma^+, 5^3\Sigma^+$	272 26, 272 21	272 06, 272 09
[Na $4s+\text{Li } 2s$ ] $4^1\Sigma^+, 4^3\Sigma^+$	254 51, 254 51	257 40, 257 12
[Na $3p+\text{Li } 2s$ ] $3^1\Sigma^+, 2^1\Pi, 3^3\Sigma^+, 2^3\Pi$	167 76, 167 29, 167 80, 167 39	169 56, 168 70
[Na $3s+\text{Li } 2p$ ] $2^1\Sigma^+, 1^1\Pi, 2^3\Sigma^+, 1^3\Pi$	151 17, 150 69, 151 17, 151 37	149 04, 149 38
[Na $3s+\text{Li } 2s$ ] $X^1\Sigma^+, 1^3\Sigma^+$	0	0

<sup>a</sup>Reference 26.<sup>b</sup>Reference 20 for  $\text{NaLi}^+$  and Ref. 6 for  $\text{NaLi}$ .

able experimental data. Similarly, generally good agreement with experimental data achieve calculations employing effective-core pseudopotentials combined with a one-electron calculations,<sup>20</sup> but comparison with many-electron CI calculations is desirable.

## II. CALCULATIONS

Multireference CI calculations<sup>21</sup> (MRDCI) have been carried out on electronic states of  $\text{NaLi}$  and  $\text{NaLi}^+$ , for different values of the internuclear distance  $R_{\text{Na-Li}}$  ranging from 2.5 to 50.0 bohr. The atomic orbital basis set employed included the aug-cc-pCVTZ basis sets for Na (Ref. 22) and Li,<sup>23</sup> obtained from the Environmental Molecular Sciences Laboratory (EMSL),<sup>24</sup> to which one  $d$  Rydberg function (exponent of 0.0032) was added to the Na basis. Furthermore, it was necessary to change the smallest  $d$  exponent of the Li basis set to 0.015, in order to improve the description of the electronic states to which Li  $3d$  contributes. The calculations employed  $C_{2v}$  symmetry, where  $\Sigma^+$  states are calculated as  $A_1$ ,  $\Pi$  states as  $B_1$  and  $B_2$ ,  $\Sigma^-$  as  $A_2$ , and  $\Delta$  as  $A_1$  and  $A_2$ . 12 states of  $^1A_1$  symmetry, 12 of  $^3A_1$ , 9  $^1B_1$ , 9  $^3B_1$ , 4  $^1A_2$ , and 4  $^3A_2$  states were calculated. Reference spaces were employed consisting of 199 configurations for the  $^1A_1$  calculations, 173 for  $^3A_1$ , 188 for  $^1B_1$ , 188 for  $^3B_1$ , 131 for  $^1A_2$ , and 131 configurations for the  $^3A_2$  calculations. As it is the standard practice in MRDCI calculations, these reference spaces were determined on the basis of preliminary calculations over the above range of values for the internuclear distance, where for each symmetry, all configurations contributing over 0.2% (in terms of the square of their coefficient in the

CI vector) are included in the reference space. In all cases, and for all states calculated at all different values of the internuclear distance, the contribution of the reference space in the final CI vector is over 97% (in terms of the sum of the squares of the coefficients of the reference configurations). Selection of configurations from the space generated by all possible single and double substitutions with respect to the reference configurations, in each calculation, was carried out with an energy threshold of 0.1  $\mu\text{hartree}$ . The resulting CI spaces had dimension between 400 000 and 600 000, at different values of  $R_{\text{Na-Li}}$ . Three-point extrapolation to zero threshold and a full-CI correction<sup>25</sup> were made to the calculated eigenvalues. For the calculations on the electronic states of  $\text{NaLi}^+$ , the reference spaces and roots calculated are 33 configurations and 15 roots for  $^2A_1$ , 20 and 9 for  $^2B_1$ , and 14 and 4 for  $^1A_2$ , while the selection threshold is 0.02  $\mu\text{hartree}$ . In all the CI calculations, only the Na  $K$  shell was kept doubly occupied and the remaining 12 electrons (11 electrons for  $\text{NaLi}^+$ ) were involved in the single and double excitations with respect to the configurations in the reference spaces. While there are only two valence electrons in the  $\text{NaLi}$  molecule (one valence electron in  $\text{NaLi}^+$ ), it is necessary to include the Na  $L$ -shell electrons and the Li  $K$ -shell electrons in the CI, as it has been shown that core-valence correlations are very significant in the alkali dimers.<sup>6</sup>

In Table I, the excitation energies calculated at the dissociation limits (i.e., at internuclear distances of 50.0 bohr for  $\text{NaLi}$  and 100.0 bohr for  $\text{NaLi}^+$ ) are compared to experimental atomic excitation energies,<sup>26</sup> for all the electronic states of  $\text{NaLi}^+$  [Table I] and of  $\text{NaLi}$  [Table I] calculated in

TABLE II. Vertical ( $\Delta E_v$ )<sup>a</sup> and adiabatic ( $T_e$ ) transition energies and dissociation energies ( $D_e$ ) for electronic states of NaLi<sup>+</sup> calculated in the present work and previously (values in brackets, from Ref. 20).

State	$\Delta E_v$ (cm <sup>-1</sup> )	$T_e$ (cm <sup>-1</sup> )	$R_{\min}$ (bohr), $D_e$ (cm <sup>-1</sup> )
X <sup>2</sup> Σ <sup>+</sup>	0	0	6.37, 8065, (6.37, 8061) $\omega_e=203.1(192.98)$ cm <sup>-1</sup>
2 <sup>2</sup> Σ <sup>+</sup>	211 15	9988 (9805) <sup>a</sup>	14.80, 322 (14.90, 294)
3 <sup>2</sup> Σ <sup>+</sup>	302 81	215 24 (215 43)	13.64, 1537 (13.65, 1423)
4 <sup>2</sup> Σ <sup>+</sup>	452 07	261 97 (262 19)	19.00, 760 (18.94, 847)
5 <sup>2</sup> Σ <sup>+</sup>	501 97	330 43 (330 11)	22.40, 2116 (22.41, 2262)
6 <sup>2</sup> Σ <sup>+</sup>	553 74	355 09 (355 75)	34.20, 177 (34.24, 265)
7 <sup>2</sup> Σ <sup>+</sup>	575 01	379 42 (···)	30.00, 811 (repulsive)
8 <sup>2</sup> Σ <sup>+</sup>	626 55	394 40 (388 96)	40.00, 205 (37.47, 375)
9 <sup>2</sup> Σ <sup>+</sup>	643 23	···	Repulsive (repulsive)
10 <sup>2</sup> Σ <sup>+</sup>	664 02	··· (402 42)	Repulsive (44.95, 127)
1 <sup>2</sup> Π	232 08	215 35 (224 71)	8.60, 782 (8.53, 496)
2 <sup>2</sup> Π	385 53	···	Repulsive (repulsive)
3 <sup>2</sup> Π	524 98	368 60 (363 19)	19.00, 2215 (19.35, 2667)
4 <sup>2</sup> Π	561 18	395 52 (388 72)	34.76, 76 (34.76, 398)
5 <sup>2</sup> Π	597 92	···	Repulsive (repulsive)
6 <sup>2</sup> Π	653 07	···	Repulsive (repulsive)
1 <sup>2</sup> Δ	483 38	··· (392 16)	Repulsive (19.59, 57)
2 <sup>2</sup> Δ	596 74	···	Repulsive (repulsive)

<sup>a</sup>At  $R_{\min}$  of the ground state.

the present work. As shown in Table I, electronic states of NaLi<sup>+</sup> up to Na 4*p* and for NaLi molecule, electronic states up to the limit Na 3*p*+Li 2*p* have been determined. The theoretical values of the excitation energy at 50.0 bohr are in very good agreement with the experimental values for the corresponding atomic excitation energies, in most cases. The largest discrepancy is found for the states of NaLi correlating with the Li 3*d* limit where the theoretical values are off by 300–660 cm<sup>-1</sup>, for different  $\Lambda S$  states. The lowest ionization energy at dissociation (i.e., the IP of Na) is calculated at 5.10 eV compared to the experimental value, 5.14 eV. The next higher ionization energy, which is the IP of Li atom is calculated at 0.28 eV above the ionic ground state limit [cf. 2038 cm<sup>-1</sup> in Table I], i.e., with a theoretical IP for Li at 5.38 eV, in good agreement with the corresponding experimental value of 5.39 eV. In addition to the experimental values, the previous theoretical values calculated by Schmidt-Mink *et al.*<sup>6</sup> for NaLi and Berriche<sup>20</sup> for NaLi<sup>+</sup> are listed for comparison. It might be noted that in the case of the cation, the near coincidence of the previous theoretical excitation energies<sup>20</sup> with the experimental [cf. Table I] is to be expected since in those calculations the cutoff radii, employed for the construction of the core-polarization potential, were optimized in order to reproduce the experimental IPs and lower atomic excited states.<sup>20</sup> Conversely, for the previous calculations on NaLi, a single cutoff parameter was used for each atom, based on the experimental IP of the atom.<sup>6</sup>

### III. RESULTS

#### A. Cation: NaLi<sup>+</sup>

The results of the calculations on NaLi<sup>+</sup> are summarized in Table II. The present results are in support of the results of the previous model potential<sup>19</sup> and pseudopotential<sup>20</sup> calculations, for the most part. As found previously, only the ground state possesses a significant minimum at  $R_{\min}$  of 6.37

bohr, with a well depth of 8065 cm<sup>-1</sup>. The excited electronic states of NaLi<sup>+</sup> are either repulsive or have very shallow minima at large internuclear distances. There are some differences between the present results and the previous,<sup>20</sup> for example, state 7 <sup>2</sup>Σ<sup>+</sup> is found here to have a minimum of 811 cm<sup>-1</sup> at 30.0 bohr, while in the most recent previous work it is listed as repulsive and, conversely, states 10 <sup>2</sup>Σ<sup>+</sup> and 1 <sup>2</sup>Δ are found here to be repulsive (cf. Table II) but were reported<sup>20</sup> as possessing shallow minima, of 127 cm<sup>-1</sup> at 44.95 bohr and 57 cm<sup>-1</sup> at 19.59 bohr respectively. Differences on such well depths cannot really be resolved as neither method of calculation can be expected to give definitive results: while the most recent previous calculations<sup>20</sup> involved full CI, it was of a rather trivial type, as only one electron was considered in the valence shell. On the other hand, the present calculations involve 11 electrons, and as a result it is not possible to carry out full-CI calculations. In both previous studies<sup>19,20</sup> on the electronic states of NaLi<sup>+</sup>, very large numbers of electronic states have been calculated with good accuracy and it would take much larger all-electron CI calculations than the present, including approaching the basis set limit, to resolve issues such as that on the existence of the above very shallow minima. Such an effort is beyond the scope of the present work. What the present work confirms is the fact that the character of the excited states is characterized by single excitations of the valence shell electron, with the inner electrons contributing to the correlation energy. In this manner, it is possible to use methods such as those of the previous studies and have good results.

#### B. Singlet and triplet electronic states of NaLi

The calculated potential energy curves of the singlet states of NaLi, correlating with dissociation limits up to Na 4*p* [cf. Table I], have been plotted in Fig. 1. As men-

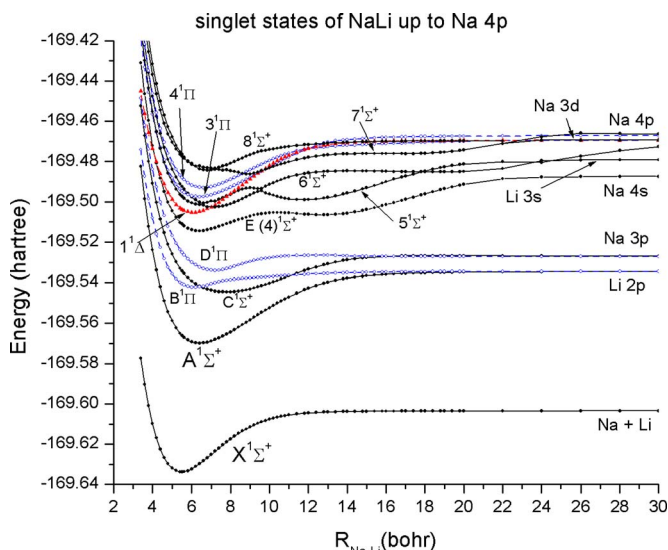


FIG. 1. (Color online) Potential energy curves of singlet spin electronic states of NaLi correlating with dissociation limits up to Na 4p+Li 2s. Solid circles:  $^1\Sigma^+$ ; open circles:  $^1\Pi$ ; solid triangles:  $^1\Delta$  states.

tioned, most of the  $^1\Sigma^+$  states (up to  $6^1\Sigma^+$ ) and the lowest two  $^1\Pi$  states (cf. Fig. 1) have been calculated previously by Schmidt-Mink *et al.*,<sup>6</sup> employing effective-core-polarization potentials and valence-CI calculations. A great deal more effort is required to reproduce those results by all-electron CI calculations such as the present work, without the effective-core-polarization potentials. The new results of the present study involve mainly the higher-lying  $^1\Sigma^+$  states, the  $^1\Delta$  states, and, in particular, the higher-lying  $^1\Pi$  states some of which (i.e.,  $3^1\Pi$ ,  $4^1\Pi$ , and  $5^1\Pi$ ) have been observed recently,<sup>17,18</sup> as well as a number of  $^3\Sigma^+$ ,  $^3\Pi$ , and  $^1\Delta$  states. Furthermore an investigation of the possible nonadiabatic interactions between the singlet states is carried out. The proximity and intermingling of the potential energy curves, especially of the higher-lying states, suggest the possibility of spectral perturbations, and for most excited states, except for  $A^1\Sigma^+$  such perturbations have been observed.<sup>10,11,13</sup> The situation is complicated further by the contribution of two charge-transfer states, corresponding to  $\text{Na}^+-\text{Li}^-$  and  $\text{Na}^--\text{Li}^+$  to the character of the  $^1\Sigma^+$  states. These ionic limits lie at 35 517 and 39 107  $\text{cm}^{-1}$ ,<sup>13</sup> and their Coulomb potentials are shown to cross the potentials  $^1\Sigma^+$  at shorter internuclear distances.<sup>10-13</sup> In the present work, it was possible to follow from large  $R$  down to 11.8 bohr, the charge-transfer character corresponding to  $\text{Na}^+-\text{Li}^-$ , which leads to a second minimum in the potential energy curve of the  $4^1\Sigma^+$  state of NaLi, and similarly for  $\text{Na}^--\text{Li}^+$  down to 11.0 bohr, which forms a second minimum in the potential energy curve of  $5^1\Sigma^+$ . The two charge-transfer states are indicated as CT in Fig. 2 where the potentials of the  $^1\Sigma^+$  states, from the third and higher, calculated in the present work have been plotted. The potentials of the  $^1\Pi$  and  $^1\Delta$  states, which have been plotted in Fig. 3, do not show any double minima, however, they do show differences from the potential energy curve of the ground state of the cation (also plotted in Fig. 3 along with the lowest excited state of the cation), implying that they are not simple Rydberg states over the different values

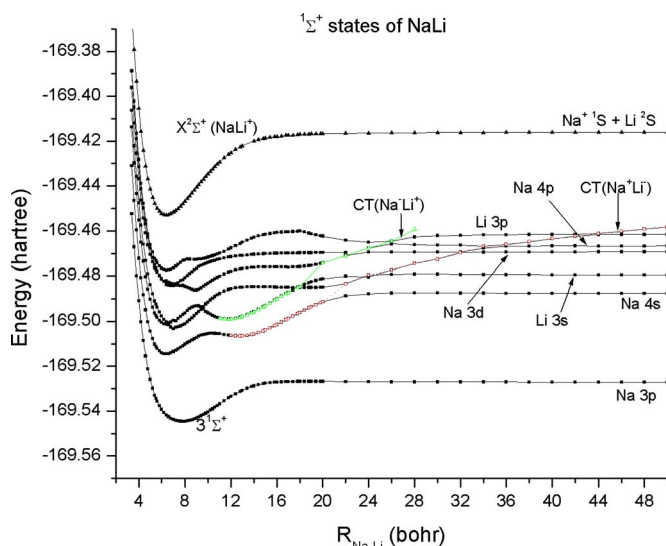


FIG. 2. (Color online) Potential energy curves of  $^1\Sigma^+$  states of NaLi. Solid squares:  $^1\Sigma^+$  states; open squares: charge-transfer state ( $\text{Na}^+\text{Li}^-$ ); open triangles: charge-transfer state ( $\text{Na}^-\text{Li}^+$ ); solid triangles:  $X^2\Sigma^+$  state of  $\text{NaLi}^+$ .

$R_{\text{Na-Li}}$  but change in character at different  $R_{\text{Na-Li}}$ , for example, changing from excited Na to excited Li character. The existence of the two ionic limits, corresponding to excited Na Rydberg states and to excited Li Rydberg states, respectively, is reflected in the shape of some of the electronic states of NaLi. For example, even the curves of the lowest two  $^1\Pi$  states,  $B^1\Pi$  and  $D^1\Pi$  (see Figs. 1 and 3) appear to be the result of such interactions between a bound and a repulsive “diabatic” potential. This of course exists for the  $^1\Sigma^+$  states as well, but it is easier to see it in the potentials of the  $^1\Pi$  states. In Table III, the results of the calculations on the singlet states are summarized and compared to available experimental data<sup>10-18</sup> and to the theoretical results of Schmidt-Mink *et al.*<sup>6</sup> for the lower-lying states. As shown in Table III, the present results are in generally good agreement with the previous theoretical and experimental results. In the present calculations, the equilibrium bond lengths are

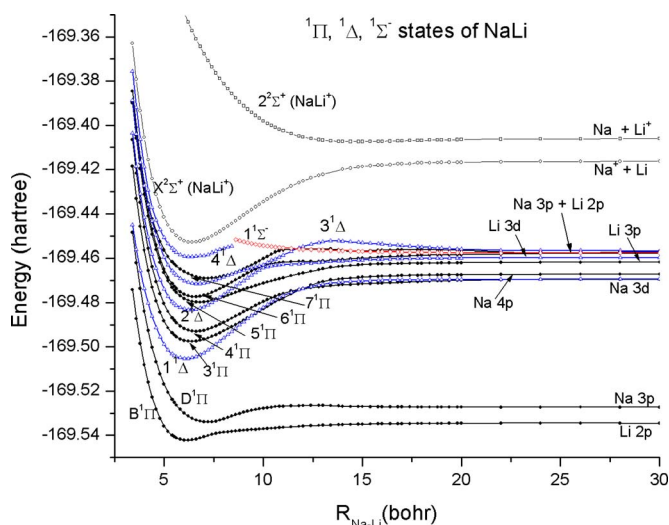


FIG. 3. (Color online) Potential energy curves of  $^1\Pi$  (solid circles),  $^1\Delta$  (open triangles), and  $^1\Sigma^-$  (open rhombi) states of NaLi, and the lowest two states of  $\text{NaLi}^+$  (open circles and open squares).

TABLE III. Vertical (at  $R_{\text{Na-Li}}$  of 5.5 bohr) ( $\Delta E_v$ ) and adiabatic ( $T_e$ ) electronic transition energies and oscillator strengths ( $f_L$ ) (at  $R_{\text{Na-Li}}$  of 5.5 bohr) and dissociation energies ( $D_e$ ) of singlet states of NaLi calculated in the present work, comparison with experimental and previous theoretical values.

State	$\Delta E_v(\text{cm}^{-1})$	$f_L^{\text{vert}}$	$T_e(\text{cm}^{-1})$	$R_{\text{min}}(\text{bohr})$	$D_e(\text{eV})$
4 $^1\Delta$	389 23	...	382 96	6.40	...
7 $^1\Pi$	375 68	0.021	361 56	7.08	0.30
3 $^1\Delta$	366 75	...	356 42	6.60	0.36
6 $^1\Pi$	353 76	0.0022	343 38 (340 41 <sup>a</sup> )	6.57 (6.41 <sup>a</sup> )	0.52 (0.54 <sup>a</sup> )
9 $^1\Sigma^+$	352 23	0.0003	34294	6.43	0.43
5 $^1\Pi$	349 89	0.0036	33792	6.76	0.49
8 $^1\Sigma^+$	345 11	0.0007	32984	7.14	0.59
7 $^1\Sigma^+$	343 15	0.0002	32377	8.90	0.53
2 $^1\Delta$	336 41	...	330 49	6.40	0.64
4 $^1\Pi$	319 87	0.007	309 04 (311 79 <sup>b</sup> )	6.60 (6.56 <sup>b</sup> )	0.70 (0.76 <sup>b</sup> )
6 $^1\Sigma^+$	310 32	0.0019	291 94, 293 13 <sup>c</sup>	6.64, 6.67 <sup>c</sup>	0.86, 0.86 <sup>c</sup>
3 $^1\Pi$	305 32	0.045	299 00 (299 82 <sup>b</sup> )	6.41, (6.30 <sup>b</sup> )	0.76 (0.78 <sup>b</sup> )
5 $^1\Sigma^+$	299 34	0.007	287 35, 290 21 <sup>c</sup> , (292 13 <sup>d</sup> )	6.96, 7.18 <sup>c</sup>	0.64, 0.65 <sup>c</sup> , (0.63 <sup>d</sup> )
1 $^1\Delta$	285 02	...	282 03	6.00	0.98
E $^1\Sigma^+$	269 15	0.001	261 84, 264 16 <sup>c</sup> , (264 74 <sup>d</sup> )	6.40, 6.3 <sup>c</sup> (6.32 <sup>b</sup> )	0.73, 0.78 <sup>c</sup> (0.78 <sup>d</sup> , 0.79 <sup>b</sup> )
D $^1\Pi$	238 46	0.019	218 95, 222 03 <sup>c</sup> , (222 62 <sup>d</sup> )	7.22, 7.10 <sup>c</sup>	0.18, 0.21 <sup>c</sup> (0.22 <sup>d</sup> )
C $^1\Sigma^+$	218 13	0.011	195 81, 195 50 <sup>c</sup> , (186 00 <sup>d</sup> , 196 11 <sup>e</sup> )	7.88, 7.81 <sup>c</sup>	0.48, 0.54 <sup>c</sup> , (0.67 <sup>d</sup> , 0.55 <sup>e</sup> )
B $^1\Pi$	204 48	0.54	200 94, 201 30 <sup>c</sup> , (200 62 <sup>d</sup> , 200 88 <sup>e</sup> )	6.12, 6.09 <sup>c</sup> , (5.89 <sup>d</sup> )	0.20, 0.23 <sup>c</sup> , (0.24 <sup>d</sup> , 0.14 <sup>d</sup> )
A $^1\Sigma^+$	148 64	0.57	140 22, 142 00 <sup>c</sup> , (141 96 <sup>d</sup> )	6.41, 6.37 <sup>c</sup>	0.96, 0.97 <sup>c</sup> (0.96 <sup>d</sup> , 0.97 <sup>e</sup> )
X $^1\Sigma^+$	0	...	...	5.48, 5.46 <sup>c</sup> , (5.45 <sup>d</sup> )	0.82, 0.87 <sup>c</sup> (0.88 <sup>d</sup> )

<sup>a</sup>Experiment (Ref. 18).<sup>b</sup>Experiment (Refs. 15–17).<sup>c</sup>Theoretical (Ref. 6).<sup>d</sup>Experiment (Refs. 10 and 11).<sup>e</sup>Experiment (Ref. 13).

slightly overestimated, while the well depths are in some cases are slightly underestimated (cf. data for the 4  $^1\Sigma^+$  state). As will be discussed below, the theoretical quantities for 6  $^1\Pi$  give a better fit for the experimental data assigned to 5  $^1\Pi$  in a recent experimental report.<sup>18</sup> The calculated oscillator strengths, at a single bond length of 5.50 bohr, i.e., at the minimum of the ground state, also given in Table III, are rather small, except for the lowest two states, indicating Rydberg character for the excited states. The present  $f$ -values are generally smaller than previously reported theoretical values,<sup>7</sup> while corresponding experimental data are not available.

As pointed out elsewhere,<sup>11–20</sup> the cation is predicted to have larger binding energy [calculated here  $D_e$  of 1.0 eV, experimental values of  $0.97 \pm 0.04$  and  $0.99 \pm 0.03$  eV (Refs. 11–20)] than the neutral NaLi [calculated here  $D_e$  of 0.82 eV, experimental of 0.88 eV (Ref. 14)] with a larger bond length ( $R_e$  of 6.37 bohr) than the neutral [calculated here  $R_e$  5.48 bohr, experimental of 5.45 bohr (Ref. 14)]. The adiabatic IP is calculated here at 4.92 eV, which is in excellent agreement with the experimental IP of  $4.94 \pm 0.10$  eV.<sup>9</sup> Similarly, the calculated vertical IP at internuclear distance of 5.50 bohr (i.e., at the ground state minimum) is 5.03 eV, while an experimental value is reported at  $5.05 \pm 0.04$  eV.<sup>11</sup> The authors<sup>11</sup> estimate their vertical IP to be about 0.06 eV larger than the adiabatic, but they have not actually determined the adiabatic IP of NaLi.

The results of the present calculations on the spin-triplet states of NaLi are summarized in Table IV, and the corresponding potential energy curves have been plotted in Fig. 4. These states have not been observed, and consequently com-

parison is only possible for those of them that have been calculated previously. The lower-lying triplet states of NaLi, (cf. Fig. 4) correlating with the lowest three dissociation limits are generally free of interactions, except for 3  $^3\Sigma^+$ , which has a local minimum as a result of an avoided crossing with 4  $^3\Sigma^+$ . The higher-lying  $^3\Sigma^+$  states have a “ladder” of avoided crossings, with the minima of the curves either close to or at an avoided crossing, indicating strong nonadiabatic interactions between these states and a repulsive state cutting through them. Similarly, the potentials of the higher-lying  $^3\Pi$  states (upper part of Fig. 4) show interactions and avoided crossings, which would lead to spectral perturbations in the triplet spectra of NaLi.

In what follows, some of the states calculated will be examined in detail, with emphasis on aspects that have not been calculated before and with reference to experimental observations.

### 1. Results on the lower-lying singlet states ( $B^1\Pi$ , $C^1\Sigma^+$ , and $D^1\Pi$ )

Besides the ground state and the A  $^1\Sigma^+$  state of NaLi, the  $B^1\Pi \rightarrow X^1\Sigma^+$  fluorescence has been investigated in great detail, and the observed intensity patterns<sup>27</sup> in the collision induced spectra have been rationalized in terms of quantum mechanical analysis<sup>28</sup> as well as physical interpretations.<sup>29</sup> Observations on the C  $^1\Sigma^+$  have been difficult<sup>11</sup> because of unfavorable overlap as the minimum of this state is displaced with respect to the ground state minimum (see Table III). Subsequent studies involving laser excitation of the B  $^1\Pi$  state and collisional energy transfer to C  $^1\Sigma^+$  have succeeded

TABLE IV. Vertical electronic transition energies ( $\Delta E_v$ ) at  $R_{\text{Na-Li}}$  of 5.50 bohrs, with respect to the ground state  $X^1\Sigma^+$  energy, adiabatic transition energies ( $T_e$ ), and dissociation energies ( $D_e$ ) of triplet electronic states of NaLi. Comparison with previous work.

State	$\Delta E_v$ (cm $^{-1}$ )	$T_e$ (cm $^{-1}$ )	$D_e$ (eV)	$R_{\text{min}}$ (bohr)
4 $^3\Delta$	369 41	358 92	0.62	6.20
7 $^3\Pi$	361 34	354 09	0.39	6.40
3 $^3\Delta$	360 54	357 31	0.36	6.80
8 $^3\Sigma^+$	355 70	338 76	0.49	6.60
6 $^3\Pi$	350 05	333 11	0.66	8.00
7 $^3\Sigma^+$	346 02	331 50	0.43	6.80
2 $^3\Sigma^+$	342 79	336 34	0.57	6.40
6 $^3\Sigma^+$	339 57	308 11, 309 27 <sup>a</sup>	0.66, 0.66 <sup>a</sup>	7.00, 6.88 <sup>a</sup>
5 $^3\Pi$	330 69	322 63	0.68	6.40
4 $^3\Pi$	323 44	293 59	0.90	7.00
5 $^3\Sigma^+$	309 72	286 33, 287 26 <sup>a</sup>	0.64, 0.69 <sup>a</sup>	7.80, 7.58 <sup>a</sup>
1 $^3\Delta^+$	296 01	291 17	0.86	6.20
3 $^3\Pi$	292 79	287 95	0.90 <sup>b</sup>	7.80 <sup>b</sup>
4 $^3\Sigma^+$	290 37	276 65 <sup>c</sup> , 281 32 <sup>a</sup>	0.51 <sup>c</sup> , 0.57 <sup>a</sup>	6.80 <sup>c</sup> , 6.55 <sup>a</sup>
3 $^3\Sigma^+$	267 78	260 52	loc. min.-repl.	6.40
2 $^3\Pi$	258 10	...	Repulsive	...
2 $^3\Sigma^+$	179 87	169 38, 172 02 <sup>a</sup>	0.59, 0.59 <sup>a</sup>	6.60, 6.52 <sup>a</sup>
1 $^3\Pi$	120 72	120 63, 122 75	1.20, 1.21 <sup>a</sup>	5.40, 5.40 <sup>a</sup>
1 $^3\Sigma^+$	9034	6533, 6841 <sup>a</sup>	0.03 <sup>a</sup>	9.00, 8.98 <sup>a</sup>

<sup>a</sup>Reference 6.

<sup>b</sup>Inner local min.

<sup>c</sup>Inner min.

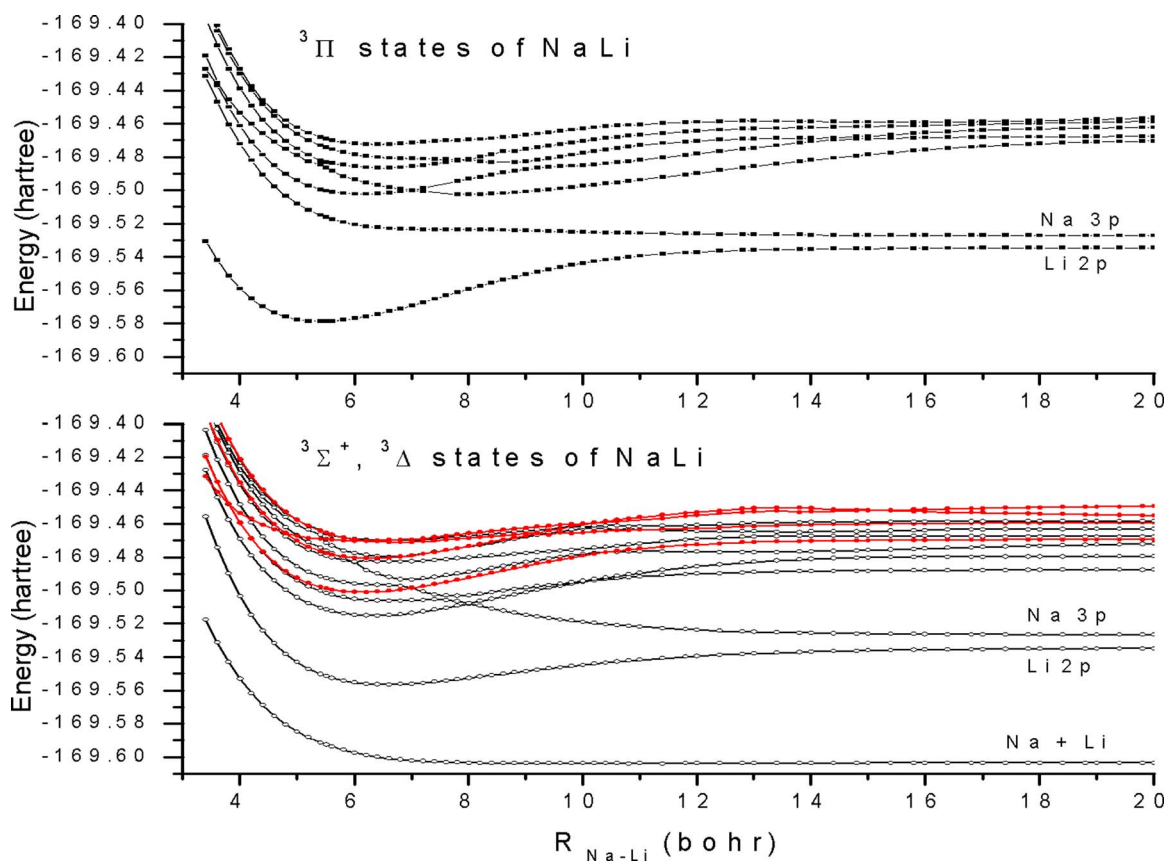


FIG. 4. (Color online) Potential energy curves of triplet states of NaLi. Lower part:  $^3\Sigma^+$  (open circles) and  $^3\Delta$  (solid circles) states. Upper part:  $^3\Pi$  states.

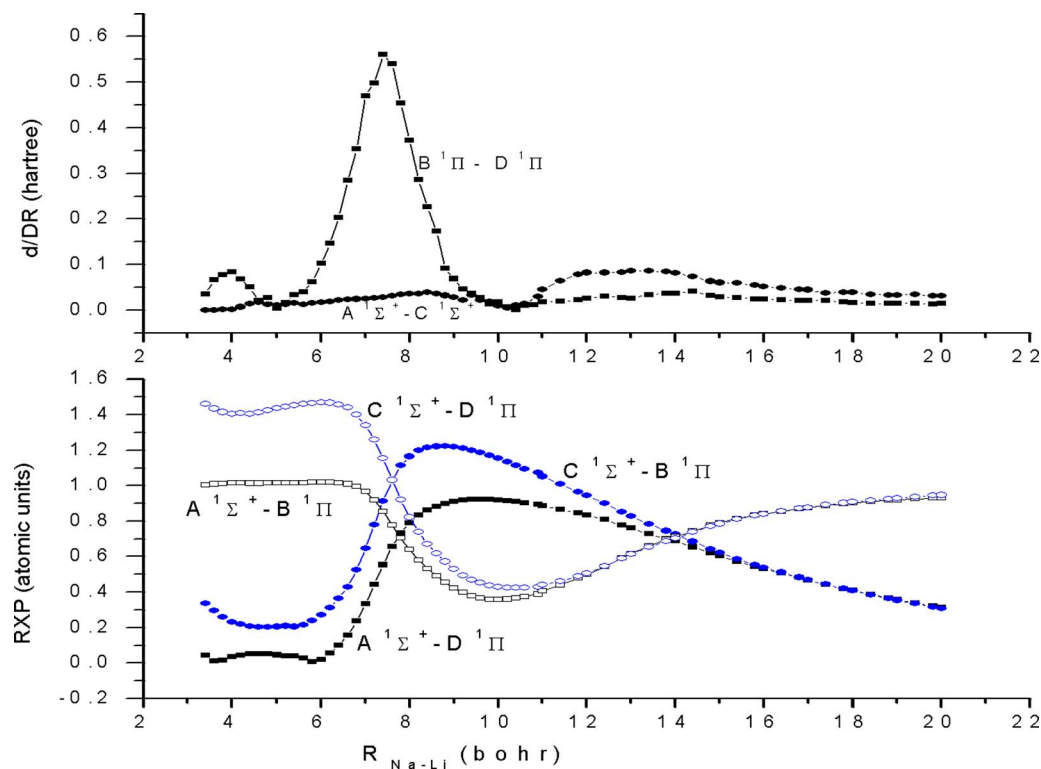


FIG. 5. (Color online) Radial coupling (upper curve) and  $r \times p$  matrix elements over pairs of electronic states:  $A^1\Sigma^+$ ,  $B^1\Pi$ ,  $C^1\Sigma^+$ , and  $D^1\Pi$ .

in observing the  $B^1\Pi \rightarrow A^1\Sigma^+$  and  $C^1\Sigma^+ \rightarrow A^1\Sigma^+$  transitions.<sup>13</sup> The authors report perturbations in the  $B^1\Pi$  and  $C^1\Sigma^+$  states at different rotational levels, which have been reduced using an effective Hamiltonian model for the interactions between these two states.<sup>13</sup> Vibrational levels calculated in the present work along with corresponding previous theoretical and experimental data may be found in the supplementary material.<sup>30</sup> Generally good agreement exists between the experimental and theoretical vibrational levels. For the  $B^1\Pi$  state experimental values exist only for the first seven levels, and for these levels the previous theoretical values are closer to the experimental than the present values. For the  $C^1\Sigma^+$  state, the present values are closer to the experimental than the previous, as also for most of the observed levels of the  $D^1\Pi$  state. The lowest  $C^1\Sigma^+$  level observed by Kappes *et al.*<sup>11</sup> at 22 814  $\text{cm}^{-1}$  (estimated as  $v' = 27 \pm 3$ ) corresponds to 2607  $\text{cm}^{-1}$  above the minimum of the  $C^1\Sigma^+$  state, using the experimental  $T_e$  and  $v_0$  of the ground state, and, according to the present results, it is the  $v=25$  level of the  $C^1\Sigma^+$  state ( $v=24$  according to the previous calculations<sup>6</sup>).

The interactions between the lower-lying states of NaLi, correlating with the two lowest excited state-dissociation limits,  $\text{Na} + \text{Li } 2p$  and  $\text{Na } 3p + \text{Li}$  [see Table I and Fig. 1] are treated in the present work by a four-state or a three-state (depending on whether  $A^1\Sigma^+$  is included or not) vibrational calculation, where the off diagonal matrix elements are the rotational-electronic coupling ( $^1\Sigma^+ - ^1\Pi$ ) and radial coupling (for  $^1\Sigma^+ - ^1\Sigma^+$  and  $^1\Pi - ^1\Pi$ ) matrix elements over the electronic wave functions, calculated at the different values of  $R_{\text{Na-Li}}$  (cf. Fig. 5). It should be noted that what is plotted in the lower part of Fig. 5 are the  $r \times p$  matrix elements (or the

matrix elements  $\langle \Psi_{el}^J(R) | L_{\pm} | \Psi_{el}^J(R) \rangle$ ) over the electronic wave functions, while the rotational-electronic interaction includes as well the factor  $1/R^2$  since it is given by  $-1/2\mu\sqrt{(J \pm \Lambda)(J + 1 \mp \Lambda)} \times \langle \Psi_{el}^J(R) | L_{\pm} | \Psi_{el}^J(R) \rangle / R^2$ , and so for large  $R$ , it becomes less important. The potential energy curves of  $B^1\Pi$  and  $D^1\Pi$  have a strongly avoided crossing near internuclear distance of 7–8 bohr (see Fig. 1), with an accompanying exchange in character. This is reflected in the peak of the  $d/dR$  matrix elements over these two states (cf. Fig. 5, upper part), and in the crossing of the  $r \times p$  coupling matrix elements of  $A^1\Sigma^+ - B^1\Pi$  and  $A^1\Sigma^+ - D^1\Pi$ , as well as in those of  $C^1\Sigma^+ - B^1\Pi$  and  $C^1\Sigma^+ - D^1\Pi$  (see Fig. 5, lower part) near 8.0 bohr. The above nonadiabatic interactions, radial and rotational electronic, will cause shifts in the positions of the rotational-vibrational levels of the  $B^1\Pi$ ,  $C^1\Sigma^+$ , and  $D^1\Pi$  states from what they would be if treated as noninteracting, while it may also cause predissociation of bound levels, which lie in the continuum of an interacting state. Predissociation widths and lifetimes have been calculated for levels of the  $B^1\Pi$ ,  $C^1\Sigma^+$ , and  $D^1\Pi$  of  $\text{Na}^7\text{Li}$ , using the method complex eigenvalue–Schrödinger equation described in detail previously,<sup>31</sup> based on complex rotation of the internuclear coordinate where the resonances are obtained as the stable complex eigenvalues, for different rotation angles. For clarity, the three-state calculations will be discussed, i.e., leaving  $A^1\Sigma^+$  out of the interacting set, as it does not affect the results significantly. The results on the perturbations of the different levels show that for  $J=1$ , only the  $B^1\Pi - D^1\Pi$  interaction is significant, causing shifts of a few wave numbers in the calculated levels of these states. It is found that vibrational levels  $v \geq 20$  of  $B^1\Pi$ , which are close to its energy at the dissociation limit, are calculated to

be broadened and correspondingly to have short predissociation lifetimes, of 9 ps ( $v=20$ ) or a fraction of 1 ps (higher levels). Therefore these levels would not be observed in emission. Similarly, vibrational levels of  $D^1\Pi$  are calculated to possess width of  $0.06\text{--}0.14\text{ cm}^{-1}$ , from  $v=6$  to  $v=13$ , and larger for higher levels. These levels are predissociated by interaction with  $B^1\Pi$  because they lie above the dissociation energy of the lower state. As the radiative lifetime of  $D^1\Pi$  is estimated at 22 ns emission from levels higher than  $v=6$  of this state would not be expected. Finally, higher vibrational levels of  $C^1\Sigma^+$ , starting at  $v=34$  and higher, are calculated to be broadened (and have short lifetime) because they lie near the dissociation limit energy of  $C^1\Sigma^+$ , even though they are below the top of the broad barrier found in the potential energy curve of this state, around internuclear distance of 30 bohr. The width of  $v=34$  is  $0.02\text{ cm}^{-1}$  and increases rapidly for  $v=35$  to  $2.8\text{ cm}^{-1}$ , which corresponds to a lifetime of about 2 ps.

For high  $J$  values, mixing of levels of  $C^1\Sigma^+$  with those of the  $^1\Pi$  states occurs. For example, for  $J=28$ , the  $v=0$  level of  $B^1\Pi$  is a linear combination  $0.1150 C^1\Sigma^+ + 0.8849 B^1\Pi$ . Conversely the  $v=6$  level of  $C^1\Sigma^+$  is, in fact,  $0.8852 C^1\Sigma^+ + 0.1148 B^1\Pi$ . The two levels are nearly degenerate with a difference in energy of only  $4\text{ cm}^{-1}$ . For  $J=29$ ,  $v=6$  of  $C^1\Sigma^+$  is lower in energy than the  $v=0$  level of  $B^1\Pi$  (again the two levels are nearly degenerate differing only by  $4.4\text{ cm}^{-1}$ ), with coefficients  $0.9002 C^1\Sigma^+ + 0.0998 B^1\Pi$  and  $0.1001 C^1\Sigma^+ + 0.8999 B^1\Pi$  for the two levels, respectively. This may give an answer to the quest for the mechanism of the  $B$ - $C$  energy transfer<sup>13</sup> since excitation of the  $v=0$ ,  $J=29$  level of  $B^1\Pi$ , which is the excitation step in the collision induced fluorescence spectra,<sup>13</sup> results in direct excitation of the  $v=6$  level of  $C^1\Sigma^+$  as well.

## 2. Results on the $E(4)^1\Sigma^+$ state

The potential energy curve of the  $4^1\Sigma^+$  shows two minima, an inner minimum of 0.73 eV at 6.40 bohr (at 6.32 bohr  $R_e$  experimental value), a barrier of 0.25 eV at 10.40 bohr (0.48 eV below the dissociation limit), and an outer minimum of 0.52 eV at 12.80 bohr. Experimental levels have been observed only for the inner minimum of  $4^1\Sigma^+$ . Previous theoretical calculations,<sup>6</sup> which have been corroborated by subsequent experimental work<sup>15,16</sup> on this state of NaLi, at least as far as the inner minimum is concerned, report the first vibrational level of the outer minimum at  $1859\text{ cm}^{-1}$  above the electronic minimum energy of this state. In the present work, the first level of the outer minimum is calculated at  $1777\text{ cm}^{-1}$ , showing that the outer minimum is calculated here at lower energy than in the previous study. The next level is calculated at 1843, a third level at 1910, and a fourth at  $1968\text{ cm}^{-1}$ . These levels are difficult to observe, as the outer minimum lies at much larger internuclear distance than the minimum of the ground state. As mentioned above (cf., CT states in Fig. 2) this outer minimum has charge-separated character,  $\text{Na}^+\text{--Li}^-$ , which is consistent with the larger  $R$  at the outer minimum than the Rydberg states.

## 3. The $3^1\Pi$ and $4^1\Pi$ states

To our knowledge there do not exist any previous theoretical calculations on the higher-lying (from  $3^1\Pi$  and up)  $^1\Pi$  states of NaLi. Spectra assigned to transitions from the ground state to  $3^1\Pi$  and  $4^1\Pi$  have been observed recently.<sup>17</sup> The present theoretical results are in agreement with the assignment of  $3^1\Pi$  and  $4^1\Pi$  to the Na  $3d$  and Na  $4p$  dissociation limits, respectively [cf. Table I]. Similarly, as shown in Table III, the calculated adiabatic transition energies,  $29\,900$  and  $30\,904\text{ cm}^{-1}$ , are in good agreement with the experimental  $T_e$  values of  $29\,982$  and  $31\,179\text{ cm}^{-1}$  for  $3^1\Pi$  and  $4^1\Pi$ , respectively, while the calculated dissociation energies for these two states are 0.70 and 0.76 eV, respectively, with the corresponding experimental  $D_e$  values at 0.78 and 0.76 eV. The present calculations obtain  $R_e$  for  $3^1\Pi$  at 6.41 bohr with experimental value at 6.30 bohr, whereas for  $4^1\Pi$  the theoretical  $R_e$  value, 6.60 bohr, is close to the experimental value, 6.56 bohr.<sup>17</sup> In Fig. 6, in the lower part the potential energy curves of the singlet states near  $3^1\Pi$  and  $4^1\Pi$ , namely,  $1^1\Delta$ ,  $5^1\Sigma^+$ ,  $6^1\Sigma^+$ , and  $7^1\Sigma^+$  are shown (as an enlargement of the upper part of Fig. 1), while in the upper part of Fig. 6, the potential energy curves of higher-lying states (from  $7^1\Sigma^+$  upwards) of NaLi have been plotted. The possibility of spectral perturbations is evident from the potential energy curves, especially for the  $3^1\Pi$  state. In fact, it has been mentioned that a number of the observed levels for this state deviate from their expected position (on the basis of a Dunham expansion) by  $0.3\text{--}0.8\text{ cm}^{-1}$ .<sup>17</sup> Such deviations are too small to pin point on the basis of the present calculations; however, it is possible to calculate the effect of nonadiabatic interactions on the theoretical unperturbed levels, by carrying out a multistate vibrational calculation, as presented above for the lower-lying states. For the  $3^1\Pi$  and  $4^1\Pi$  states, the vibrational calculation involves five of the states shown in the lower section of Fig. 6 (omitting  $7^1\Sigma^+$ ), the radial coupling matrix elements over the different  $R_{\text{Na--Li}}$  values, between states of the same  $\Lambda$  symmetry, and the rotational-electronic coupling matrix elements between states differing in  $\Lambda$  by 1. As noted above, the rotational-electronic coupling, which increases with increasing rotational quantum number, is not very significant, especially for low  $J$  values as the  $R_e$  of all these states is quite large and the interaction varies as  $1/R^2$ . Indeed, the multistate vibrational calculations show small ( $0.2\text{--}0.9\text{ cm}^{-1}$ ) shifts downward of the vibrational levels of  $3^1\Pi$  and similarly small shifts ( $0.2\text{--}0.7\text{ cm}^{-1}$ ) upward in the vibrational levels of  $4^1\Pi$  from those calculated in the absence of the interactions. These shifts are independent of the  $J$  level considered, from  $J=2$  to  $J=35$ , implying that the effect is solely due to the radial coupling between the two  $^1\Pi$  states.

The radial coupling interaction between the  $5^1\Sigma^+$  and  $6^1\Sigma^+$  states is quite complex, and vibrational levels of these states have contributions from both states and large shifts, between 4 and  $12\text{ cm}^{-1}$  in the vibrational levels. For large  $J$

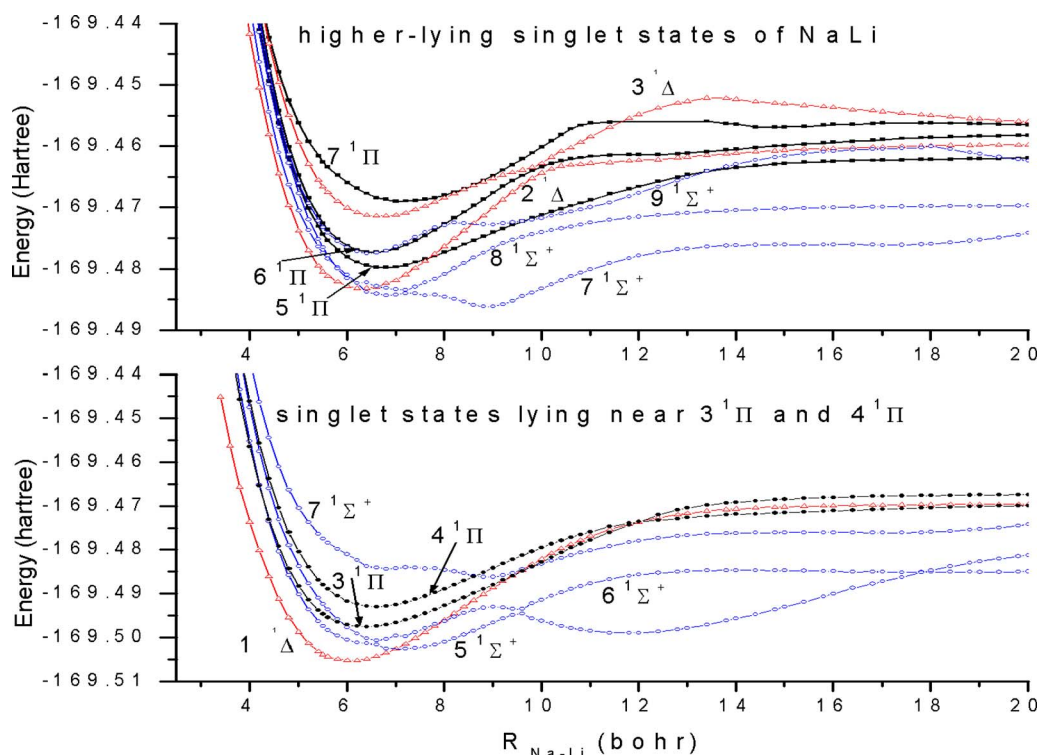


FIG. 6. (Color online) Lower part: Potential energy curves of electronic states in the region of and interacting with  $3^1\Pi$  and  $4^1\Pi$ . Upper part: higher-lying electronic states of NaLi.

values, there is mixing of the vibrational levels of the  $^1\Sigma^+$  states with those of  $3^1\Pi$ , and to a lesser extent of  $4^1\Pi$ , when there is near coincidence of the unperturbed levels, without accompanying shifts in the levels of the  $^1\Pi$  states, beyond those mentioned above. Finally, the  $1^1\Delta$  state is totally unaffected and has no effect on the levels of the two  $^1\Pi$  states.

As shown in Fig. 6, the adiabatic potential energy curves of  $3^1\Pi$  and  $4^1\Pi$  states of NaLi have an avoided crossing at internuclear distance of 12.0 bohr, where the two curves come to near coincidence. So in terms of diabatic (i.e., crossing) states,  $3^1\Pi$  correlates with Na  $4p$  and  $4^1\Pi$  with Na  $3d$ . However, we might point out that these labels are rather formal as at the minimum the two states both have mixed Rydberg  $p$  and Rydberg  $d$  character. Even so, we can use the *ab initio* potential energy curves for these two diabatic Rydberg states  $4p$  and  $3d$  and the ground state of the cation to calculate quantum-defect functions and in turn generate potential energy curves for all the higher  $nd$  and  $(n+1)p$  Rydberg states up to the first ionic limit. Again we will not reproduce the method here as it has been given in detail elsewhere.<sup>31,32</sup> Since the interaction between these two states at the avoided crossing is not significant (as shown by their near coincidence at the avoided crossing), the  $3d$  and  $4p$  states are treated separately. The quantum-defect functions  $\eta(R)$  (Refs. 31 and 32) are obtained as analytic fits of the values calculated at different values of  $R$ , from 3.4 to 20.0 bohr, using a polynomial expansion  $\eta_i(R) = \sum_{j=0}^4 a_j R^j$ , where the coefficients  $a_j$  are  $-0.128\ 949$ ,  $-0.175\ 669$ ,  $0.023\ 325$ ,  $-0.000\ 947$ , and  $0.000\ 011$  for the  $3d$  and  $1.106\ 842$ ,  $-0.561\ 594$ ,  $0.075\ 836$ ,  $-0.004\ 138$ , and  $0.000\ 080$  for the  $4p$  expansion. The quantum-defect functions thus obtained

may be employed to generate all higher  $nd$  and  $(n+1)p$  Rydberg states of NaLi. As the next higher  $^1\Pi$  states obtained from the CI calculations correlate either with excited Li atom limits ( $5^1\Pi$ ,  $6^1\Pi$ ) or with excited both Na and Li ( $7^1\Pi$ ), see Table I, they do not formally fall in the above two Rydberg series. However,  $6^1\Pi$  coincides with the  $4d$  diabatic state obtained from the quantum-defect analysis at short  $R$ . Similarly at some  $R$  values  $7^1\Pi$  coincides with the  $4d$ , while at  $R > 15$  bohr the potential energy curve of  $9^1\Pi$  with a theoretical dissociation limit energy at  $34\ 135\ \text{cm}^{-1}$  (experimental Na  $4d$  energy at  $34\ 549\ \text{cm}^{-1}$ ) coincides with the quantum-defect derived  $4d$  state. States  $9^1\Pi$  and  $8^1\Pi$  of NaLi have not been included in the presentation of the results as they have not been determined very well at short internuclear distances. While Rydberg states characterized by excitation in Na converge to (and follow the shape of) the lowest electronic state of the cation,  $X^2\Sigma^+$ , Rydberg states characterized by Li\* converge to the second ionic limit,  $2^2\Sigma^+$ , which is repulsive (see Fig. 3). Thus as mentioned above the higher-lying adiabatic  $^1\Pi$  states are indeed combinations of different types of states, combining the curves of the different ionic limits at different regions of  $R$ , resulting in potential energy curves with complicated structure. A more comprehensive quantum-defect treatment would involve making use of diabatic states and their interaction matrix elements in a multichannel quantum-defect treatment, including as well both ionic limits, to determine all the adiabatic potential energy curves up to the ionic limits.<sup>32</sup> Such an undertaking may be considered for future work on this system.

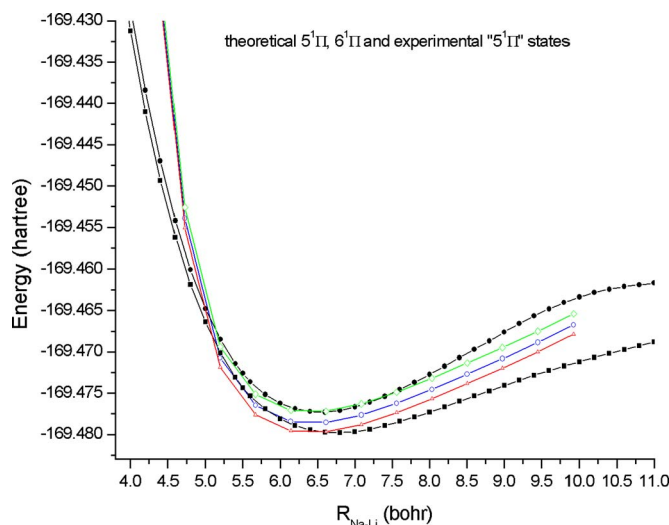


FIG. 7. (Color online) Potential energy curves for  $5^1\Pi$  and  $6^1\Pi$  of the present work and IPA curve of Bang *et al.* (Ref. 18). Open circles: IPA curve with respect to the minimum of the ground state; open triangles: IPA in coincidence with  $5^1\Pi$ ; and open rhombi: IPA placed in coincidence with  $6^1\Pi$ .

#### 4. The $5^1\Pi$ and $6^1\Pi$ states

The next higher  $^1\Pi$  state above  $4^1\Pi$  observed by Bang *et al.*<sup>18</sup> has been assigned as  $5^1\Pi$ , correlating with Na  $3s^2S$  and Li  $3d^2D$ .<sup>18</sup> However,  $5^1\Pi$  correlates with Na  $3s^2S$  + Li  $3p^2P^o$  [cf. Table I] dissociation limits. The theoretical adiabatic transition energy of  $5^1\Pi$  from the ground state minimum is  $33\,792\text{ cm}^{-1}$ , which is in good agreement with the experimental  $T_e$  of  $34\,041\text{ cm}^{-1}$ , but the difference between the theoretical  $R_e$  (6.76 bohr) and the experimental value (6.41 bohr) for  $5^1\Pi$  is much bigger than for any of the other states calculated. The origin of this discrepancy in  $R_e$  by 0.35 bohr is not clear as there is no obvious reason why the theoretical value for this state should be any worse than those of the other  $^1\Pi$  states. However, the next higher  $^1\Pi$  state calculated,  $6^1\Pi$ , does correlate with Na  $3s^2S$  + Li  $3d^2D$ , it has a smaller  $R_e$  value, 6.57 bohr, which is larger than the experimental by 0.16 bohr, and with transition energy of  $34\,338\text{ cm}^{-1}$ , i.e.,  $297\text{ cm}^{-1}$  larger than the experimental, and theoretical dissociation energy of 0.52 eV with experimental  $D_e$  for the observed state at 0.54 eV. Therefore, according to the present results, the spectroscopic constants derived from the observed spectrum by Bang *et al.*<sup>18</sup> would fit better the  $6^1\Pi$  state calculated here. This is also shown pictorially in Fig. 7 where, along with the *ab initio* potential energy curves for  $5^1\Pi$  (solid squares) and  $6^1\Pi$  (solid circles), the inverted perturbation approach (IPA) potential of Bang *et al.*<sup>18</sup> derived from the observed spectra has been plotted. The open circles are the IPA potential with respect to the ground state minimum, open triangles the IPA potential shifted to fit the  $T_e$  value of  $5^1\Pi$ , and open rhombi the IPA potential shifted to fit  $6^1\Pi$ . As shown in Fig. 7, a better fit is obtained by the IPA potential with  $6^1\Pi$ , at least near the bottom of the well. At short distances, where the theoretical curves for  $5^1\Pi$  and  $6^1\Pi$  are very close, the IPA

curve, which appears to rise more rapidly than the theoretical, is only a reasonable extension of the potential based on the experimental levels, which lies between 5.20 and 8.50 bohr.<sup>33</sup>

#### IV. CONCLUSION

In the present work *ab initio* MRDCI calculations have been presented on electronic states of NaLi and NaLi<sup>+</sup>, in an effort to provide theoretical information on states of NaLi that had not been calculated previously but have been observed, as well as to compare many-electron CI results with those of methods involving polarization core potentials and valence CI, which have been particularly successful for both NaLi (Ref. 6) and NaLi<sup>+</sup>.<sup>19,20</sup> Furthermore, the effect of nonadiabatic interactions between the different states has been investigated both for the lower-lying and higher-lying states of NaLi. The present study shows that for the neutral molecule, the present results are in good agreement with the experimental and those of the previous theoretical study<sup>6</sup> where available, while it is difficult to reproduce the excellent agreement with experiment of the core-polarization-two-electron CI results.<sup>6</sup> Similarly for NaLi<sup>+</sup> it would take a much bigger theoretical undertaking in order to resolve differences between the previous core-polarization-one-electron CI calculations and the present 11-electron (for the cation) CI. The present calculations on the recently observed  $3^1\Pi$  and  $4^1\Pi$  states of NaLi are in good agreement with experiment, while the theoretical results assign to  $6^1\Pi$  the next higher  $^1\Pi$  state observed.<sup>18</sup> Finally, nonadiabatic effects are important, especially for the higher-lying  $^1\Sigma^+$  states but also for the  $^1\Pi$ . Radial coupling is more significant in causing shifts in the vibrational levels, while rotational-electronic coupling is not, since it varies as  $1/R^2$  and in this molecule rather large  $R_e$  are found. However, when there is near coincidence of the vibrational levels of states differing in  $\Lambda$  by 1, the rotational-electronic coupling leads to mixing of these states, as found, for example, for the  $J=29$  level of  $v=0$  of  $B^1\Pi$  and  $v=6$  of  $C^1\Sigma^+$ , consistent with the observed transfer of energy from  $B^1\Pi$  to  $C^1\Sigma^+$  upon excitation of the above level of  $B^1\Pi$ .<sup>13</sup> All the *ab initio* energies of the present study are available from EPAPS.

#### ACKNOWLEDGMENTS

Partial support of this work through the “Excellence in the Research Institutes” program, supervised by the General Secretariat for Research and Technology/Ministry of Development, Greece (Phase I and II, Project Nos. 64769 and 2005ΣΕ01330081), is gratefully acknowledged. The authors are grateful to Professor Pawel Kowalczyk for helpful communications.

<sup>1</sup>P. J. Bertocini, G. Das, and A. C. Wahl, *J. Chem. Phys.* **52**, 5112 (1970).

<sup>2</sup>S. Green, *J. Chem. Phys.* **54**, 827 (1971).

<sup>3</sup>P. Rosmus and W. Meyer, *J. Chem. Phys.* **65**, 492 (1976).

<sup>4</sup>A. I. Boldyrev, J. Simons, and P. von R. Schleyer, *J. Chem. Phys.* **99**, 8793 (1993).

<sup>5</sup>W. Müller and W. Meyer, *J. Chem. Phys.* **80**, 3311 (1984).

<sup>6</sup>I. Schmidt-Mink, W. Müller, and W. Meyer, *Chem. Phys. Lett.* **112**, 120 (1984).

<sup>7</sup>M. Merawa, D. Begue, and A. Dargelos, *Chem. Phys. Lett.* **372**, 529

- (2003).
- <sup>8</sup>M. M. Hessel, *Phys. Rev. Lett.* **26**, 215 (1971).
- <sup>9</sup>K. F. Zmbov, C. H. Wu, and H. R. Ihle *J. Chem. Phys.* **67**, 4603 (1977).
- <sup>10</sup>F. Engelke, G. Ennen, and K. H. Meiwes, *Chem. Phys.* **66**, 391 (1982).
- <sup>11</sup>M. M. Kappes, K. O. Marti, P. Radi, M. Schar, and E. Schumacher, *Chem. Phys. Lett.* **107**, 6 (1984).
- <sup>12</sup>C. E. Fellows, *J. Mol. Spectrosc.* **136**, 369 (1989).
- <sup>13</sup>C. E. Fellows, J. Vergès, and C. Amiot, *J. Chem. Phys.* **93**, 6281 (1990).
- <sup>14</sup>C. E. Fellows, *J. Chem. Phys.* **94**, 5855 (1991).
- <sup>15</sup>W. Jastrzebski, P. Kowalczyk, R. Nadyak, and A. Pashov, *Spectrochim. Acta, Part A* **58**, 2193 (2002).
- <sup>16</sup>N. H. Bang, W. Jastrzebski, and P. Kowalczyk, *J. Mol. Spectrosc.* **233**, 290 (2005).
- <sup>17</sup>N. H. Bang, A. Grochola, W. Jastrzebski, and P. Kowalczyk, *Chem. Phys. Lett.* **440**, 199 (2007).
- <sup>18</sup>N. H. Bang, A. Grochola, W. Jastrzebski, and P. Kowalczyk, "Spectroscopy of mixed alkali in dimers by the polarization labeling technique: Application to NaLi and NaRb molecules," *Opt. Mater.* (in press).
- <sup>19</sup>S. Magnier and M. Aubert-Frécon, *J. Phys. Chem. A* **105**, 165 (2001).
- <sup>20</sup>H. Berriche, *J. Mol. Struct.: THEOCHEM* **663**, 101 (2003).
- <sup>21</sup>R. J. Buenker, in *Studies in Physical and Theoretical Chemistry, Current Aspects of Quantum Chemistry*, edited by R. Carbo (Elsevier, Amsterdam, 1981), Vol. 2, p. 17; R. J. Buenker and R. A. Phillips, *J. Mol. Struct.: THEOCHEM* **123**, 291 (1985); R. J. Buenker and S. Krebs, in *Recent Advances in Multireference Methods*, edited by K. Hirao (World Scientific, Singapore, 1999), p. 1.
- <sup>22</sup>D. E. Woon and T. H. Dunning, Jr. (unpublished).
- <sup>23</sup>T. H. Dunning, Jr., *J. Chem. Phys.* **90**, 1007 (1989).
- <sup>24</sup>See <http://gnode2.pnl.gov/bse/portal> for Environmental Molecular Sciences Laboratory (EMSL).
- <sup>25</sup>S. R. Langhoff and E. R. Davidson, *Int. J. Quantum Chem.* **8**, 61 (1974).
- <sup>26</sup>Yu. Ralchenko, A. E. Kramida, J. Reader, and NIST ASD Team, NIST Atomic Spectra Database (Version 3.1.4), National Institute of Standards and Technology, Gaithersburg, MD, 2008, available (<http://physics.nist.gov/asd3>).
- <sup>27</sup>C. R. Vidal and M. M. Hessel, *J. Appl. Phys.* **43**, 2776 (1972).
- <sup>28</sup>Ch. Ottinger, *Chem. Phys.* **1**, 161 (1973).
- <sup>29</sup>D. Poppe, *Chem. Phys. Lett.* **19**, 63 (1973).
- <sup>30</sup>See EPAPS Document No. E-JCPSA6-129-633829 for eight tables of data of which seven are the calculated total energies of the electronic states of NaLi and one calculated vibrational levels of the lower-lying states. For more information on EPAPS, see <http://www.aip.org/pubservs/epaps.html>.
- <sup>31</sup>I. D. Petsalakis, G. Theodorakopoulos, Y. Li, G. Hirsch, R. J. Buenker, and M. S. Child, *J. Chem. Phys.* **108**, 7607 (1998).
- <sup>32</sup>I. D. Petsalakis, G. Theodorakopoulos, and M. S. Child, *J. Phys. B* **28**, 5179 (1995).
- <sup>33</sup>P. Kowalczyk (private communication).